[9] W. E. Dixon, E. Zergeroglu, D. M. Dawson, and B. T. Costic, "Repetitive learning control: A Lyapunov-based approach," *IEEE Trans. Syst., Man, Cybern. B, Cybern.*, vol. 32, no. 4, pp. 538–545, Aug. 2002.
[10] M. Sun, Y. Chen, and B. Huang, "Robust higher order iterative learning algorithm for tracking control of delayed repeated systems," (in Chinese) *Acta Automatica Sinica*, vol. 20, pp. 360–365, 1994.
[11] J.-X. Xu and Z. Qu, "Robust iterative learning control for a class of nonlinear systems," *Automatica*, vol. 34, no. 8, pp. 983–988, 1998.
[12] P. Lucibello and S. Panzieri, "Cyclic control of linear systems with application to a flexible arm," *Inst. Elect. Eng. Proc.*, vol. 145, pt. D, pp. 19–24, Jan. 1998.
[13] G. Oriolo, S. Panzieri, and G. Ulivi, "An iterative learning controller for nonholonomic mobile robots," *Int. J. Robot. Res.*, vol. 17, no. 9, pp. 954–970, 1998.
[14] M. W. Spong and M. Midyasagar, *Robot Dynamics and Control*. New York: Wiley, 1989.
[15] F. L. Lewis, C. T. Abdallah, and D. M. Dawson, *Control of Robot Manipulators*. New York: Macmillan, 1993.
[16] S. S. Ge and C. C. Hang, "Structural network modeling and control of rigid body robots," *IEEE Trans. Robot. Autom.*, vol. 14, no. 5, pp. 823–826, Oct. 1998.
[17] S. S. Ge, T. H. Lee, and C. J. Harris, *Adaptive Neural Network Control of Robotic Manipulators*. London, U.K.: World Scientific, Dec. 1998.
[18] F. L. Lewis, S. Jagannathan, and A. Yesildirek, *Neural Network Control of Robot Manipulators and Nonlinear Systems*. London, U.K.: Taylor & Francis, 1999.
[19] M. French and E. Rogers, "Non-linear iterative learning by an adaptive Lyapunov technique," *Int. J. Control*, vol. 73, no. 10, pp. 840–850, 2000.
[20] M. Norrlof, "An adaptive iterative learning control algorithm with experiments on an industrial robot," *IEEE Trans. Robot. Autom.*, vol. 18, no. 2, pp. 245–251, Apr. 2002.
[21] T. Y. Kuc and J. S. Lee, "An adaptive learning control of uncertain robotic systems," in *Proc. 30th IEEE Conf. Decision, Control*, 1991, pp. 1206–1211.
[22] J. Y. Choi and J. S. Lee, "Adaptive iterative learning control of uncertain robotic systems," *Inst. Elect. Eng. Proc.*, vol. 147, no. 2, pt. D, pp. 217–223, 2000.
[23] P. B. Goldsmith, "On the equivalent of causal LTI iterative learning control and feedback control," *Automatica*, vol. 38, pp. 703–708, 2002.

Dynamics and Balance of a Humanoid Robot During Manipulation Tasks

Kensuke Harada, Shuuji Kajita, Kenji Kaneko, and Hirohisa Hirukawa

***Abstract*—In this paper, we analyze the balance of a humanoid robot during manipulation tasks. By defining the *generalized zero-moment point (GZMP)*, we obtain the region of it for keeping the balance of the robot during manipulation. During manipulation, the convex hull of the supporting points forms the 3-D convex polyhedron. The region of the GZMP is obtained by considering the infinitesimal displacement and the moment about the edges of the convex hull. We show that we can determine whether or not the robot may keep balance for several styles of manipulation tasks, such as pushing and pulling an object. The effectiveness of our proposed method is demonstrated by simulation.**

***Index Terms*—Dynamical balance, humanoid robot, object manipulation, zero-moment point (ZMP).**

NOMENCLATURE

We use the following nomenclature in this paper.

Σ_R	Reference coordinate frame fixed to the sole of the robot's foot.
Σ_i	Coordinate frame fixed at the center of gravity of the ith $(i = 1, \ldots, n)$ link of the robot.
$\boldsymbol{p}_{Hj} = \begin{bmatrix} x_{Hj} \\ y_{Hj} \\ z_{Hj} \end{bmatrix}$	Position vector of the contact point between the jth hand and the object $(j = 1, 2)$.
$\boldsymbol{p}_{Fj} = \begin{bmatrix} x_{Fj} \\ y_{Fj} \\ z_{Fj} \end{bmatrix}$	Position vector of a point included in the contact surface between the jth foot and the ground $(j = 1, 2)$.
$\boldsymbol{f}_{Hj} \in R^3$	Reaction force of the jth hand.
$\boldsymbol{\tau}_{Hj} \in R^3$	Reaction torque of the jth hand about $\boldsymbol{p}_{Hj}$.
$\boldsymbol{f}_{Fj} \in R^3$	Reaction force of the jth foot.
$\boldsymbol{\tau}_{Fj} \in R^3$	Reaction torque of the jth foot about $\boldsymbol{p}_{Fj}$.
$\boldsymbol{c}_i \in R^3$	Position vector of the origin of Σ_i.
$m_i \in R^1$	Mass of the link i.
$I_i \in R^{3\times 3}$	Inertia tensor of the link i.
$\boldsymbol{\omega}_i \in R^3$	Angular velocity vector of the link i.

Manuscript received December 22, 2004; revised July 1, 2005 and September 9, 2005. This paper was recommended for publication by Associate Editor Q. Huang and Editors I. Walker and F. Park upon evaluation of the reviewers' comments. This work was performed under the Basic Technology Research Promotion Program, R&D on Basic Technology for Humanoid Robots Working in Real Environments of NEDO, FY2002-2006. This paper was presented in part at the IEEE/RSJ International Conference on Intelligent Robots and Systems, 2003.

The authors are with the National Institute of Advanced Industrial Science and Technology, Tsukuba 305-8568, Japan (e-mail: kensuke.harada@aist.go.jp).

Digital Object Identifier 10.1109/TRO.2006.870649

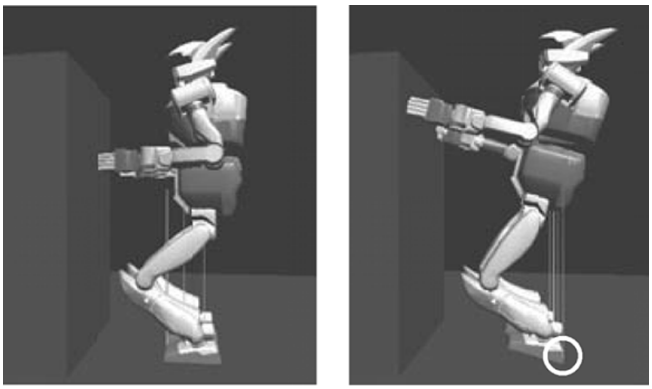

(a) (b)

Fig. 1. Examples of pushing task. (a) Pushing with small pushing force. (b) Pushing with large pushing force.

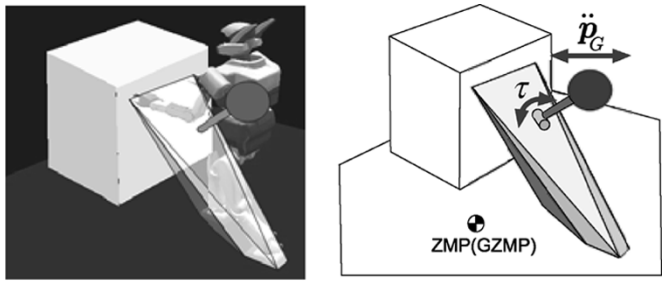

(a) (b)

Fig. 2. Explanation of our proposed method. (a) 3-D convex hull of supporting points. (b) The moment about an edge of the convex hull.

$\boldsymbol{p}_G = \begin{bmatrix} x_G \\ y_G \\ z_G \end{bmatrix}$	Position vector of the center of gravity of the robot defined by $\boldsymbol{p}_G = \sum_{i=1}^{n} m_i \boldsymbol{c}_i / \sum_{i=1}^{n} m_i$.
$\boldsymbol{p}_E = \begin{bmatrix} x_E \\ y_E \\ z_E \end{bmatrix}$	Position vector of the generalized zero-moment point (GZMP).
$\boldsymbol{f}_E \in R^3$	Reaction force of the robot.
$\boldsymbol{\tau}_E \in R^3$	Reaction torque of the robot about the GZMP.

I. Introduction

Humanoid robots are expected to work in the environments structured for humans. However, the research studies on manipulation by a humanoid are limited. For the purpose of enhancing the manipulation capability of a humanoid robot, this paper studies the balance of a humanoid robot considering the interaction between the hand and the environment.

Without considering the interaction between the hands and the environment, the zero-moment point (ZMP) [1] has been widely used for biped/quadruped robots to be able to walk stably on a flat floor. As an example of manipulation by a humanoid robot, Fig. 1 shows a humanoid robot pushing a wall. As shown in Fig. 1(a), if the robot pushes a wall with small pushing force, the face contact between the feet and the floor can be kept. On the other hand, if the pushing force increases, only the heel may contact the floor, as shown in Fig. 1(b). However, the balance can be kept even when only the heel contacts the floor. Defining the ZMP as the COP of contact between the feet and the floor, this means that the balance can be kept even when the ZMP exists on the edge of the foot-supporting area. Since we cannot determine whether or not the robot keeps balance by using this ZMP, we consider generalizing the ZMP as the COP, also including the contact between the hands and the environment.

When a hand contacts the environment as shown in Fig. 2, the convex hull of the supporting points forms a 3-D convex polyhedron. For simplicity, let us consider modeling the robot using a massless convex polyhedron and a mass connected with the polyhedron through the joints [Fig. 2(b)]. Here, if the acceleration is small, the convex polyhedron will maintain its initial posture. However, if the acceleration becomes larger, the convex polyhedron might rotate about an edge, and the robot may fall down.

By defining the ZMP, considering the interaction between the hand and the environment as the GZMP, we obtain the region of the GZMP in this research. If the GZMP is included strictly inside this region, the robot keeps balance. The region will be obtained by using the following algorithm.

1) We calculate both the infinitesimal displacement of the constrained convex polyhedron and the moments about every edge of it. Then we check whether or not the convex polyhedron might rotate around an edge of it.
2) By calculating the change of moment about an edge, we check whether or not the convex polyhedron will return to the initial posture after starting to rotate about the edge.
3) By projecting the edge of the convex polyhedron onto the floor, the region of GZMP is obtained.

Here, steps 1) and 2) are required, since the region of the GZMP changes according to the kinematic and dynamic conditions for the 3-D convex polyhedron.

In this paper, after discussing the previous studies, we define the GZMP in Section III. After Section IV, we mainly focus on the GZMP and obtain the region of the GZMP for maintaining the balance of the robot. By considering the mobility and the moment about an edge of the 3-D convex polyhedron, we show that the region can be obtained on the floor. In Section V, we show simulation results.

II. Relevant Work

Balance of a Multilegged Robot: As for the indexes for biped/quadruped walking robots to maintain their dynamical balance, ZMP was introduced [1]. The ZMP has been very commonly used for the gait planning of biped humanoid robots, such as in [10]–[13]. When a humanoid robot walks on a flat floor, the ZMP is always included in the 2-D convex hull of the foot-supporting area, since it is equivalent to the center of pressure (COP). On the other hand, Goswami [2] proposed the foot rotation indicator (FRI) point, enabling monitoring the severity of the gait's instability.

To ensure a quadruped robot walks stably on a sloped surface, several indexes have been proposed [3]–[6]. While the ZMP is commonly used for biped/quadruped robots, the research studies on ZMP analysis during manipulation tasks are limited. Kitagawa *et al.* [7] proposed using the ZMP on the sloped plane during manipulation tasks.

Humanoid Robots: Since Honda Motors developed its P2 humanoid robot [10], much research on humanoid robots has been done [11]–[13]. However, the research studies on manipulation by a humanoid robot are limited, except for [8] and [14]–[17], though manipulation is necessary for a humanoid robot to work in a real environment.

So far, there has been no research on the ZMP applicable for several types of manipulation tasks.

Maintenance of Contact: Form closure and force closure are known indexes for a mechanical system to maintain a given motion without breaking contact. In robotics, both indexes have been mainly used to constrain an object grasped by a robotic hand [18]–[20]. In the field of

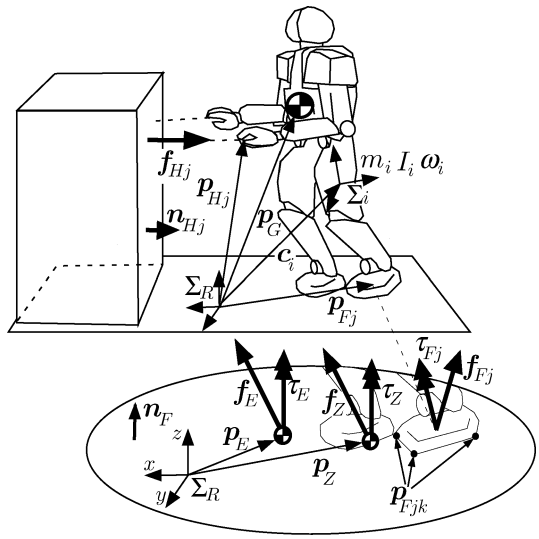

Fig. 3. Model of the system.

assembly, the stability of an object placed on a jig under gravity was studied [23].

III. Definition of GZMP

A. Assumptions

Fig. 3 shows a model of the humanoid robot studied in this paper. We imposed the following assumptions:

1) we consider a humanoid robot standing/walking on a flat floor, where at least one of the hands contacts the environment;
2) the hand does not grasp, but simply touches, the environment;
3) the friction forces at all contact points of the robot are small enough.

Assumption 3 is imposed because if the internal force exists under the frictional contacts, it becomes difficult to determine the internal force uniquely for a given motion of the robot.

B. GZMP

We first define the GZMP on the floor. However, we will introduce the virtual plane and extend the definition of the GZMP on the virtual plane[1] in the next section.

Definition 1 (GZMP on the Floor): The GZMP is the point on the floor at which the tangential components of the moment $\boldsymbol{\tau}_E = [\tau_{Ex}\ \tau_{Ey}\ \tau_{Ez}]^T$ generated by the reaction force/moment are zero, i.e., $\tau_{Ex} = \tau_{Ey} = 0$. The reaction force and moment are generated by the inertial force and the gravity force.

The reaction force $\boldsymbol{f}_E$ and moment $\boldsymbol{\tau}_E$ at the GZMP are expressed as follows:

$$\boldsymbol{f}_E = M(\ddot{\boldsymbol{p}}_G - \boldsymbol{g}) \tag{1}$$

$$= \sum_{j=1}^{2}(\boldsymbol{f}_{Hj} + \boldsymbol{f}_{Fj}) \tag{2}$$

$$\boldsymbol{\tau}_E = \dot{\boldsymbol{L}}_G + M(\boldsymbol{p}_G - \boldsymbol{p}_E) \times (\ddot{\boldsymbol{p}}_G - \boldsymbol{g}) \tag{3}$$

$$= \sum_{j=1}^{2}\left\{(\boldsymbol{p}_{Hj} - \boldsymbol{p}_E) \times \boldsymbol{f}_{Hj} + (\boldsymbol{p}_{Fj} - \boldsymbol{p}_E) \times \boldsymbol{f}_{Fj} + \boldsymbol{\tau}_{Fj}\right\} \tag{4}$$

[1]We do not restrict the virtual plane to be parallel to the real floor.

where $M = \sum_{i=1}^{n} m_i$, $\boldsymbol{g} = [0\ 0\ -g]^T$, and $\boldsymbol{L}_G (= [L_{Gx}\ L_{Gy}\ L_{Gz}]^T)$ denote the mass of the object, the gravity vector, and the angular momentum about the center of gravity of the robot, as defined by

$$\boldsymbol{L}_G = \sum_{i=1}^{n}\{m_i(\boldsymbol{p}_i - \boldsymbol{p}_G) \times \dot{\boldsymbol{c}}_i + \boldsymbol{I}_i\boldsymbol{\omega}_i\} \tag{5}$$

respectively.

The position of the GZMP can be obtained by substituting $\tau_{Ex} = \tau_{Ey} = 0$ into (3) and solving with respect to $\boldsymbol{p}_E$

$$x_E = \frac{-\dot{L}_{Gy} + Mx_G(\ddot{z}_G + g) - M(z_G - z_E)\ddot{x}_G}{M(\ddot{z}_G + g)} \tag{6}$$

$$y_E = \frac{\dot{L}_{Gx} + My_G(\ddot{z}_G + g) - M(z_G - z_E)\ddot{y}_G}{M(\ddot{z}_G + g)}. \tag{7}$$

When the hand does not contact the environment, the ZMP is equivalent to the COP of the foot–ground contact. However, when the hand contacts the environment, the GZMP is different from the COP of the foot–ground contact, and may exist outside of the foot-supporting area. Here, Takenaka [9] considered the ZMP during manipulation as the COP of the foot–ground contact.

IV. Region of GZMP

A. Convex Hull

In this section, we obtain the region of GZMP by considering both the infinitesimal displacement of the constrained convex polyhedron and the moment about the edges of it. Also, the region is defined on the floor by introducing the method for projecting the GZMP.

We will explain our proposed method using the 3-D convex polyhedron shown in Fig. 4(a). Since the robot will rotate about an edge of the convex hull when falling down, we focus on the rotational motion of the convex polyhedron about the edge, including the vertices X and Y. Let $\boldsymbol{p}_{\rm rot}$ be the position vector of an arbitrary point on the line including the vertices X and Y. Also, let $\Delta\boldsymbol{q}_{\rm rot} = [\Delta\boldsymbol{q}_{\rm rot}^T\ \Delta\boldsymbol{\theta}_{\rm rot}^T]^T$ be the infinitesimal translational/rotational displacement vector of the convex polyhedron. Since the vertex Z may break contact with the environment but it cannot go inside it, the following inequality can be satisfied:

$$\boldsymbol{d}_j^{(XY)}\Delta\boldsymbol{q}_{\rm rot} \geq 0, \quad (j = 1, \ldots, L) \tag{8}$$

where

$$\boldsymbol{d}_j^{(XY)} = \begin{bmatrix} \boldsymbol{n}_j \\ (\boldsymbol{p}_j - \boldsymbol{p}_{\rm rot}) \times \boldsymbol{n}_j \end{bmatrix}^T$$

$$\Delta\boldsymbol{q}_{\rm rot} = \begin{bmatrix} \Delta\boldsymbol{p}_{\rm rot}^T & \Delta\boldsymbol{\theta}_{\rm rot}^T \end{bmatrix}^T$$

$\boldsymbol{p}_j$ $(j = 1, \ldots, L)$ denotes the position vector of the contact points between the environment and the vertices except for X and Y, and $\boldsymbol{n}_j$ $(j = 1, \ldots, L)$ denotes the unit normal vector of the environment contacting the jth vertex. When the convex hull rotates about the edge including the vertices X and Y, we can define

$$\Delta\boldsymbol{p}_{\rm rot} = \boldsymbol{0} \tag{9}$$

$$\Delta\boldsymbol{\theta}_{\rm rot} = \frac{\boldsymbol{p}_X - \boldsymbol{p}_Y}{\|\boldsymbol{p}_X - \boldsymbol{p}_Y\|}\Delta\theta \tag{10}$$

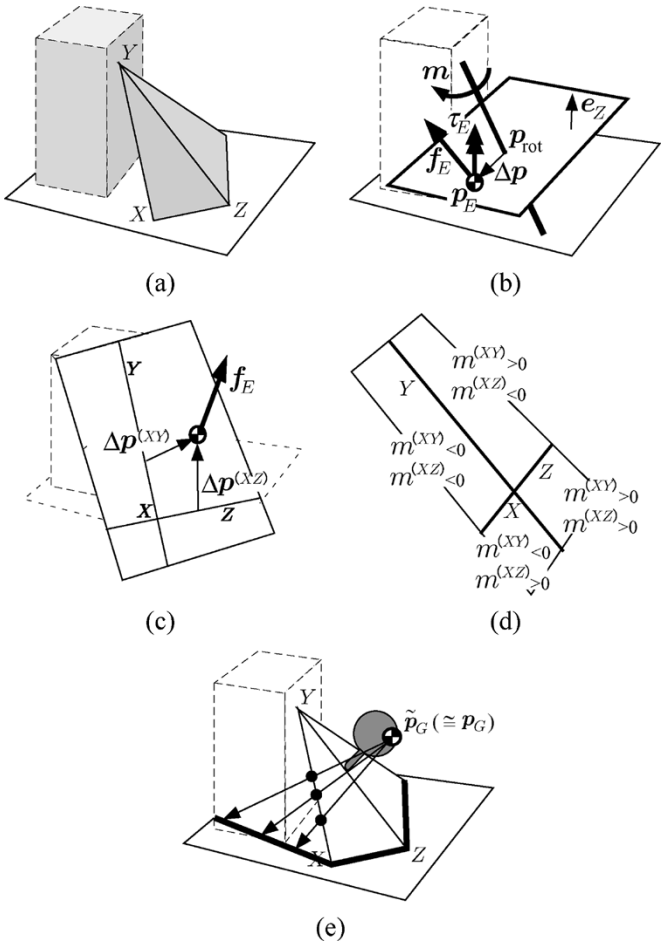

Fig. 4. Convex-polyhedron-based method. (a) Convex hull of contact points. (b) Rotation around a segment of convex hull. (c) Plane including two edges. (d) Region of ZMP. (e) Stable region.

where $\Delta\theta$ denotes the scalar variable expressing the infinitesimal rotational displacement about the edge. Substituting (9) and (10) into (8) and aggregating for $j = 1, \ldots, L$, we obtain the following inequality:

$$\boldsymbol{d}^{(XY)}\Delta\theta > 0 \tag{11}$$

where

$$\boldsymbol{d}^{(XY)} = \begin{bmatrix} \{(\boldsymbol{p}_1 - \boldsymbol{p}_{\rm rot}) \times \boldsymbol{n}_1\}^T \\ \vdots \\ \{(\boldsymbol{p}_L - \boldsymbol{p}_{\rm rot}) \times \boldsymbol{n}_L\}^T \end{bmatrix} \frac{\boldsymbol{p}_X - \boldsymbol{p}_Y}{\|\boldsymbol{p}_X - \boldsymbol{p}_Y\|}.$$

By taking (11) into consideration, the following proposition can be obtained.

Proposition 1 (Feasible Edge of the Convex Hull): If all the elements of $\boldsymbol{d}^{(XY)}$ in (11) are positive or negative, the convex hull might rotate about the edge including the vertices X and Y.

B. Moment About an Edge

Due to the reaction force applied to the convex hull, the moment will be generated about an edge of the convex hull. In this subsection, we will obtain the relationship between the GZMP and the moment about an edge of the convex hull.

By using the duality between the force and the infinitesimal displacement, the moment about the edge including the vertices X and Y satisfies the following equation:

$$m^{(XY)} = \boldsymbol{d}^{(XY)T}\boldsymbol{k}, \quad \boldsymbol{k} \geq 0. \tag{12}$$

If *Proposition 1* is satisfied, (12) shows that the sign of $m^{(XY)}$ is same as that of $\Delta\theta$.

Then, to obtain the relationship between the GZMP and the moment about an edge of the convex polyhedron, we introduce a virtual plane and define the GZMP on the plane as shown in Fig. 4(b). By using the force $\boldsymbol{f}_E$ and moment $\boldsymbol{\tau}_E$ at the GZMP on the virtual plane, we can also formulate the moment about the edge including the vertices X and Y as

$$m^{(XY)} = \frac{\boldsymbol{p}_X^T - \boldsymbol{p}_Y^T}{\|\boldsymbol{p}_X - \boldsymbol{p}_Y\|}\left((\boldsymbol{p}_E - \boldsymbol{p}_{\rm rot}) \times \boldsymbol{f}_E + \boldsymbol{e}_Z\boldsymbol{e}_Z^T\boldsymbol{\tau}_E\right) \tag{13}$$

where $\boldsymbol{e}_Z$ denotes the unit normal vector of the virtual plane. When $(\boldsymbol{p}_X - \boldsymbol{p}_Y)^T\boldsymbol{e}_Z \neq 0$ is satisfied in (13), $\boldsymbol{\tau}_E$ affects the moment about the edge. In this case, the direction of the moment about the edge cannot be uniquely determined by simply considering the position of the GZMP on the virtual plane. On the other hand, $(\boldsymbol{p}_X - \boldsymbol{p}_Y)^T\boldsymbol{e}_Z = 0$ is satisfied when two vertices X and Y are included in the virtual plane. Thus, to determine the rotation of the convex polyhedron by considering the position of the GZMP on the virtual plane, the virtual plane should be defined to include the edge of the convex polyhedron. Thus, using the edge of the convex polyhedron, we show the definition of the GZMP on the virtual plane as follows.

Definition 2 (GZMP on the Virtual Plane): The GZMP $\boldsymbol{p}_E^{(XY)} = [x_E^{(XY)}\ y_E^{(XY)}\ z_E^{(XY)}]^T$ is the point on the virtual plane at which the components of the moment $\boldsymbol{\tau}_E$ tangential to the virtual plane including the vertices X and Y are zero. Here, the edge of the convex hull including the vertices X and Y satisfies *Proposition 1*.

Using this definition, we can determine the direction of moment about an edge by considering the position of the GZMP on the virtual plane. Let the unit vector expressing the direction of $\boldsymbol{\tau}_E$ be $\boldsymbol{e}_z^{(XY)}$, and the two unit vectors normal to $\boldsymbol{e}_z^{(XY)}$ be $\boldsymbol{e}_x^{(XY)}$ and $\boldsymbol{e}_y^{(XY)}$. When the virtual plane is expressed as $z_E^{(XY)} = z_{Ed}^{(XY)}$, the position of the GZMP modified in *Definition 2* can be expressed as

$$\begin{bmatrix} x_E^{(XY)} \\ y_E^{(XY)} \end{bmatrix} = -\{M\boldsymbol{E}[(\ddot{\boldsymbol{p}}_G - \boldsymbol{g}) \times \boldsymbol{D}]\}^{-1} \times \left\{M\boldsymbol{E}\left(\boldsymbol{p}_G - \boldsymbol{e}z_{Ed}^{(XY)}\right) \times (\ddot{\boldsymbol{p}}_G - \boldsymbol{g}) + \boldsymbol{E}\dot{\boldsymbol{L}}_G\right\} \tag{14}$$

where

$$\boldsymbol{E} = [\boldsymbol{e}_x^{(XY)}\ \boldsymbol{e}_y^{(XY)}]^T$$
$$\boldsymbol{D} = \begin{bmatrix} 1 & 0 & 0 \\ 0 & 1 & 0 \end{bmatrix}^T$$
$$\boldsymbol{e} = [0\ 0\ 1]^T.$$

Now, the virtual plane is divided into two regions, using the line including the edge where each region is identified by the direction of moment about the edge. However, since the direction of moment about an edge satisfying *Proposition 1* is unique, the GZMP is included in one of the two regions on the virtual plane. Then, let us consider the virtual plane including two edges sharing a common vertex, as shown in Fig. 4(c). By using two lines, we divide the virtual plane into four regions. The four regions on the virtual plane can be identified by the direction of moment about two edges, as shown in Fig. 4(d). If both of the edges satisfy *Proposition 1*, the GZMP is included in one of the

four regions. Fig. 4(c) shows the region of the GZMP corresponding to $m^{(XY)} > 0$ and $m^{(XZ)} < 0$. Also, Fig. 4(d) shows the four regions on the plane defined by the vertices X, Y, and Z.

Furthermore, let us consider the motion of the convex hull after the convex hull begins rotating about the edge including the vertices X and Y. Let us observe the motion of the robot from the reference coordinate system fixed to its sole. The direction of the gravity force changes due to the rotation about the edge. This change of gravity force vector affects the moment about the edge. To explain the basic mechanism as simply as possible, let us suppose that an inverted pendulum moves from the unstable equilibrium state. In such a case, the pendulum will be accelerated due to the moment about the fulcrum generated by the gravity force. On the other hand, when the pendulum moves from the stable equilibrium state, the pendulum will decelerate due to the moment about the fulcrum generated by the gravity force. The infinitesimal change of the moment about the edge including the vertices X and Y caused by the change of gravity force vector can be expressed by

$$\begin{aligned}\Delta m^{(XY)} &= -M\frac{\boldsymbol{p}_X^T-\boldsymbol{p}_Y^T}{\|\boldsymbol{p}_X-\boldsymbol{p}_Y\|}(\boldsymbol{p}_G-\boldsymbol{p}_{\rm rot})\times\{(\boldsymbol{R}_{-\Delta\theta}-\boldsymbol{I}_3)\boldsymbol{g}\}\\ &= M\frac{\boldsymbol{p}_X^T-\boldsymbol{p}_Y^T}{\|\boldsymbol{p}_X-\boldsymbol{p}_Y\|^2}(\boldsymbol{p}_G-\boldsymbol{p}_{\rm rot})\times\{(\boldsymbol{p}_X-\boldsymbol{p}_Y)\times\boldsymbol{g}\}\,\Delta\theta\\ &\triangleq L^{(XY)}\Delta\theta \end{aligned} \tag{15}$$

where $\boldsymbol{R}_{-\Delta\theta}$ denotes the rotation matrix about the edge including the vertices X and Y, whose amount of rotation is $-\Delta\theta$, and $\boldsymbol{I}_3$ denotes the 3×3 identity matrix. Since the sign of $\Delta\theta$ is same as that of $m^{(XY)}$, the rotational velocity will increase when the convex hull begins rotating if the sign of $\Delta m^{(XY)}$ is different from that of $\Delta\theta$. Therefore, we can introduce the following proposition.

Proposition 2 (Change of Moment About an Edge): For an edge of the convex hull satisfying *Proposition 1*, the angular velocity will increase when the convex hull begins to rotate, if $L^{(XY)} < 0$ is satisfied.

If the convex hull decelerates after it begins rotating, the robot may not necessarily fall down, even if the ZMP is on the edge of the region, as shown in the next subsection.

C. Projection

In this subsection, we define the region of the GZMP on the floor. For this purpose, we first project the GZMP defined in the virtual plane onto the real floor.

We first introduce a vector $\tilde{\boldsymbol{p}}_G(=[\tilde{x}_G\ \tilde{y}_G\ \tilde{z}_G]^T)$, and consider the change of coordinates between $\boldsymbol{p}_G$ and $\tilde{\boldsymbol{p}}_G$ defined by

$$-\frac{\dot{L}_{Gy}}{M}+x_G(\ddot{z}_G+g)-(z_G-z_E)\ddot{x}_G=\tilde{x}_G(\ddot{\tilde{z}}_G+g)-(\tilde{z}_G-z_E)\ddot{\tilde{x}}_G \tag{16}$$

$$\frac{\dot{L}_{Gx}}{M}+y_G(\ddot{z}_G+g)-(z_G-z_E)\ddot{y}_G=\tilde{y}_G(\ddot{\tilde{z}}_G+g)-(\tilde{z}_G-z_E)\ddot{\tilde{y}}_G \tag{17}$$

$$\tilde{z}_G=z_G. \tag{18}$$

Applying the change of coordinates to (6) and (7), the position of the GZMP can be defined as follows:

$$x_E=\frac{\tilde{x}_G(\ddot{\tilde{z}}_G+g)-(\tilde{z}_G-z_E)\ddot{\tilde{x}}_G}{\ddot{\tilde{z}}_G+g} \tag{19}$$

$$y_E=\frac{\tilde{y}_G(\ddot{\tilde{z}}_G+g)-(\tilde{z}_G-z_E)\ddot{\tilde{y}}_G}{\ddot{\tilde{z}}_G+g}. \tag{20}$$

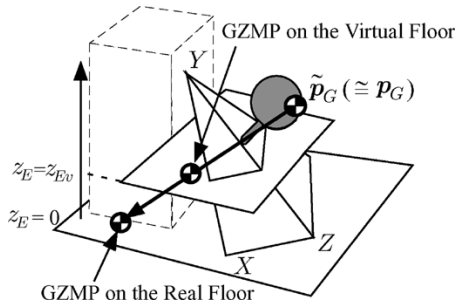

Fig. 5. Projection of the GZMP.

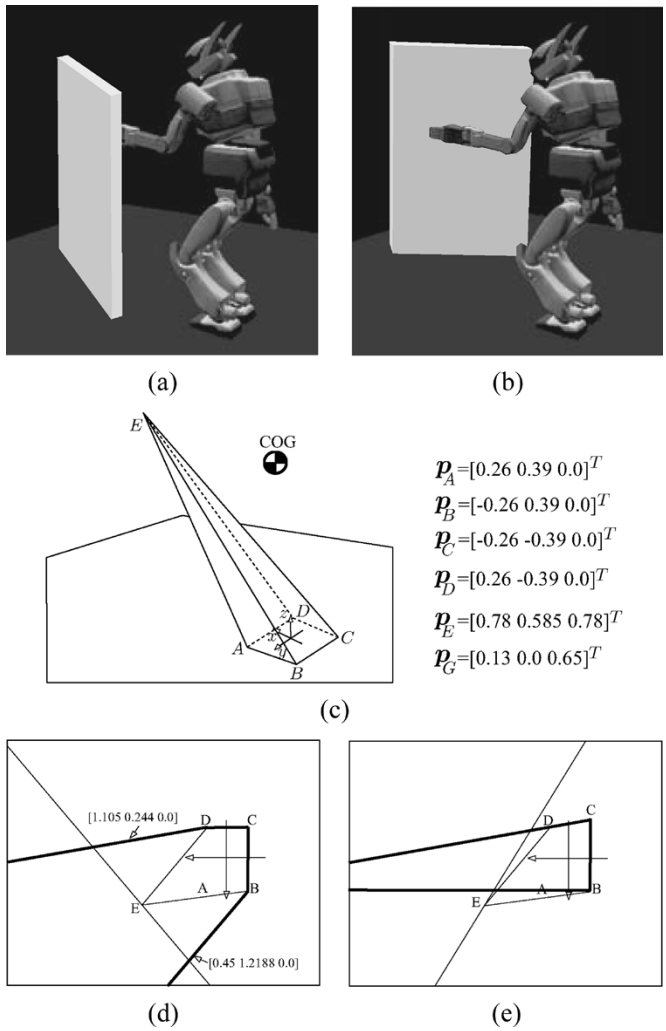

Fig. 6. Numerical examples 1 and 2. (a) The hand contacts an object in the left side (example 1). (b) The hand contacts an object in the right side (example 2). (c) The convex hull of supporting points. (d) Result of example 1. (e) Result of example 2.

Note that (19) and (20) are the same as those of an inverted pendulum. The following proposition can be held for the projection of the GZMP included in a virtual plane onto the real floor (Fig. 5).

Proposition 3 (Projection of GZMP): Draw a line including both $\tilde{\boldsymbol{p}}_G(z_E=z_G)$ and the GZMP on the virtual floor. The intersection of the line and the real floor corresponds to the GZMP on the real floor.

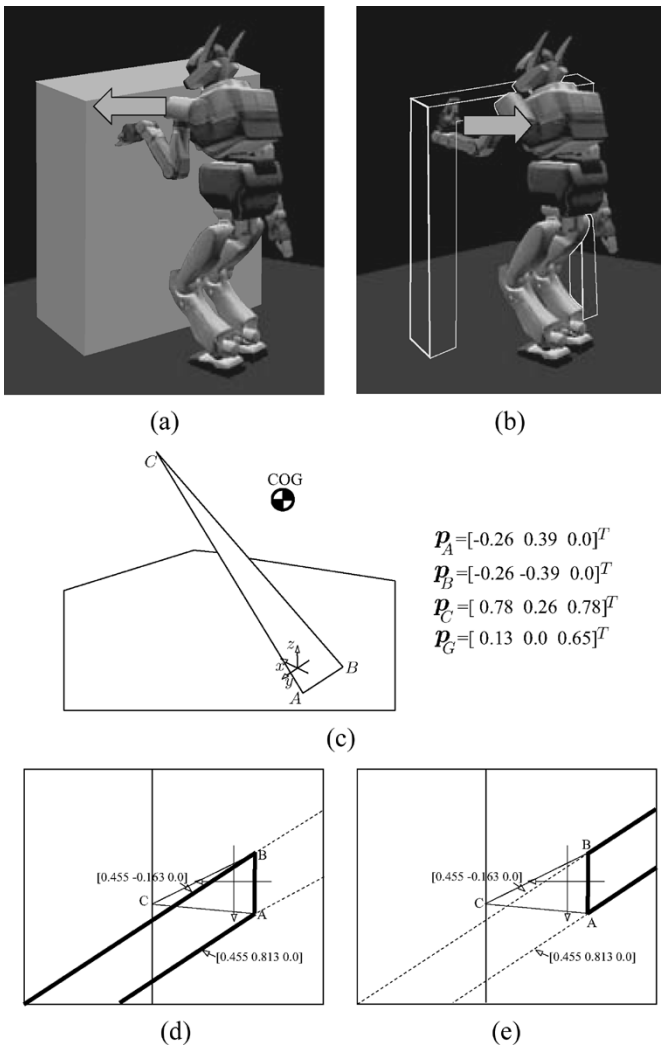

Fig. 7. Numerical examples 3 and 4. (a) Pushing an object (example 3). (b) Pushing an object (example 4). (c) The convex hull of supporting points. (d) Result of example 3. (e) Result of example 4.

Proof: In (19) and (20), the GZMP is concentrated on a single point

$$\tilde{\boldsymbol{p}}_G(z_E = z_G) = \begin{bmatrix} x_G - \frac{\dot{L}_{Gy}}{(M(\ddot{z}_G+g))} \\ y_G + \frac{\dot{L}_{Gx}}{(M(\ddot{z}_G+g))} \\ z_G \end{bmatrix} \tag{21}$$

when $z_E = \tilde{z}_G$. Moreover, (19) and (20) are linear equations with respect to $\boldsymbol{p}_E$. Therefore, since all points on the line including both $\tilde{\boldsymbol{p}}_G(z_E = z_G)$ and the GZMP on the virtual floor can be the GZMP, we confirm the theorem is correct.

Using *Proposition 3*, we project the line including the edges of the convex hull satisfying *Proposition 1* onto the real floor, and the lines projected on the floor form the edge of the region of the GZMP. Here, since (21) depends on the position of the COG of the robot, the region of the GZMP also depends on the position of the COG.

Now, the method for obtaining the region of the GZMP for maintaining the balance of a humanoid robot is summarized by the following theorem.

Theorem 1 (Region of GZMP): Project all the edges of the convex hull satisfying *Proposition 1* onto the floor using *Proposition 3*, as shown in Fig. 4(e). The region of the GZMP is defined by the direction of moment about an edge using (12). If *Proposition 2* is satisfied, the robot might fall down when the GZMP lies on the edge of the region.

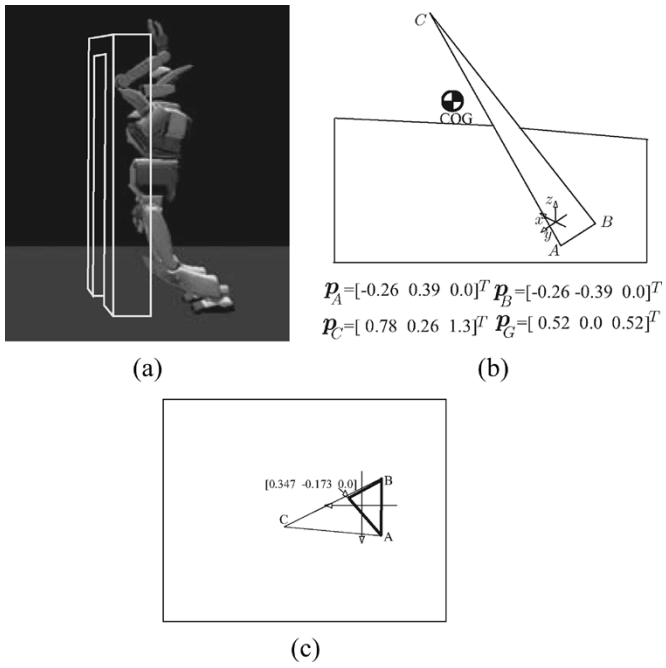

Fig. 8. Numerical example 5. (a) Leaning on an object (example 5). (b) The convex hull of supporting points. (c) Result of example 5.

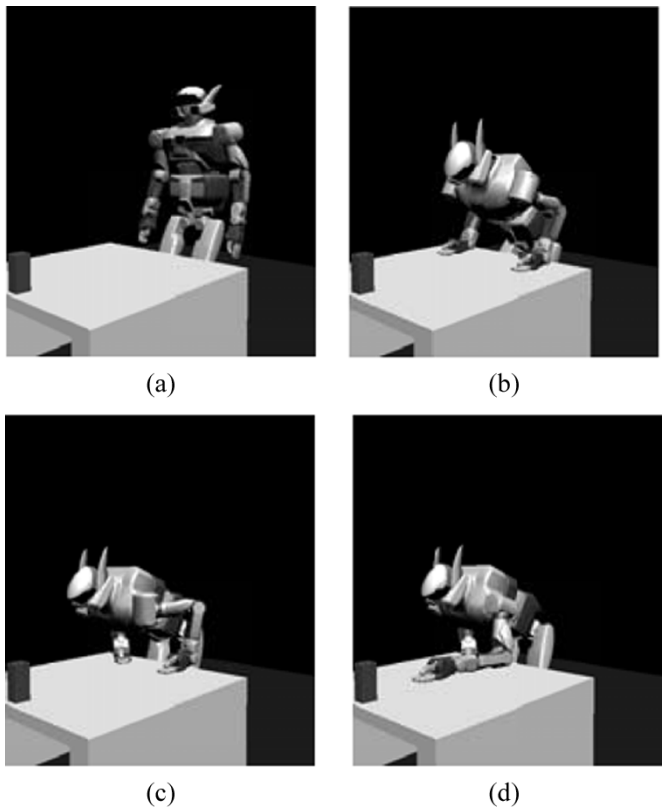

Fig. 9. Simulation result where balance is maintained. (a) $t = 0.18$ s. (b)$t = 8.20$ s. (c) $t = 10.9$ s. (d) $t = 13.6$ s.

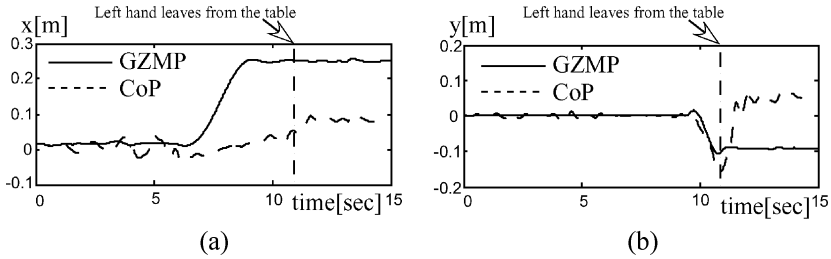

Fig. 10. GZMP and COP of the foot–ground contact. (a) GZMP and COP of foot–ground contact in x-direction. (b) GZMP and COP of foot–ground contact in y-direction.

D. Discussion

Motion of the Object: Let us consider the case where a humanoid robot pushes an object placed on the floor and where the weight of the object is light. In such a case, the robot may fall down as the object moves away from the robot. To prevent the robot from falling down, the COP of the foot–ground contact should be included in the 2-D convex hull of the foot-supporting area. For the COP of the foot–ground contact to be included in the 2-D convex hull of the foot-supporting area, the hand reaction force should be adequately taken into consideration. On the other hand, in this paper, we consider the region of the GZMP defined in *Definition 1* on the floor. We consider the case where the humanoid robot falls down by rotating about an edge of the 3-D convex hull of the supporting points.

Friction Force: In this research, we formulated the region of GZMP assuming the friction force small enough. However, in actual situations, we cannot ignore the effect of friction force. Stability of the robotic manipulation under frictional contact has been looked into by some researchers, such as Lynch [21]. He classified the motion of the object into two sets, i.e., 1) the object always keeps the contact with the robot; and 2) the object may break the contact with the robot. By extending our proposed method to frictional contacts, we expect that the region of GZMP can also be classified into two sets. Recently, Harada *et al.* [22] formulate the GZMP considering the effect of friction. Different from the method proposed in this paper, the region of the ZMP was obtained by using the numerical calculation. The region of the GZMP obtained in this method gives a necessary condition for keeping balance of the robot.

V. Simulation

A. Direction of Normal Vector

We first consider the examples which image is shown in Fig. 6(a) and (b).[2] In both cases, the shapes of the convex hull of the supporting points are assumed to be same [Fig. 6(c)]. The difference between (a) and (b) is the direction of the normal vector of the object surface at the contact point between the object and the hand. In (a) and (b), the hand contacts an object on the left side and on the right side, respectively.

By calculating $\boldsymbol{d}^{(XY)}$, we can prove from *Proposition 1* that the convex hull shown in Fig. 6(a) might rotate about the edges BC, CD, DE, and EB, but cannot rotate about the edges AD, AE, AB, and CE. On the other hand, the convex hull shown in Fig. 6(b) might rotate about the edges AB, BE, BC, and DE, but cannot rotate about the edges CD, AD, AE, and CE. Assuming $\ddot{\boldsymbol{p}}_G = [1.2\ 1.2\ 0]^T$ and $\dot{\boldsymbol{L}}_G = \boldsymbol{0}$, we show the region of the GZMP using the bold lines in Fig. 6(c) and (d). These results match our intuition where, if the left hand is supported by the object on the left side, the region of the GZMP is extended to the left.

[2]Since Fig. 6(a) and (b) show the image of the robot's configurations, the numerical values of Fig. 6(c) do not always correspond to those of Fig. 6(a) and (b).

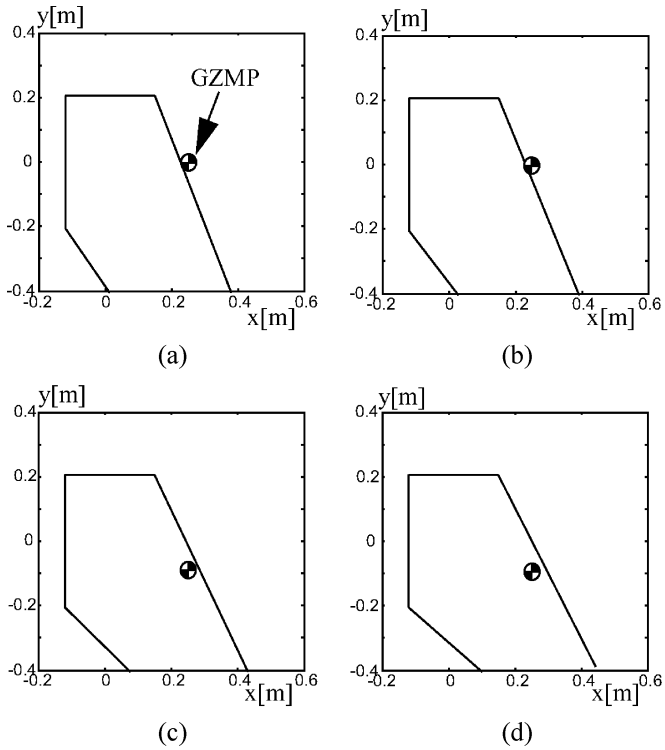

Fig. 11. GZMP and its region (the region was obtained without considering the interaction between the left hand and the table). (a) GZMP in $x-y$ plane ($t = 9.5$ s). (b) GZMP in$x-y$ plane ($t = 10.0$ s). (c) GZMP in $x-y$ plane ($t = 10.5$ s). (d) GZMP in $x-y$ plane (= 11.0 s).

B. Pushing and Pulling

Next, we consider the examples whose images are shown in Fig. 7(a) and (b), where a humanoid robot respectively pushes and pulls an object. For simplicity, we assume that each foot makes the point contact with the ground. The shape of the convex hull of the supporting points is shown in Fig. 7(c). The difference between (a) and (b) is the direction of the normal vector of the object surface at the contact point between the hand and the object. In this case, due to the difference of the direction of the normal vector, the direction of moment about the edge $m^{(\mathrm{AB})}$ differs in the two examples. Hence, the region of the GZMP can be obtained as shown by the bold lines in Fig. 7(d) and (e).

C. Leaning on an Object

We further consider the example shown in Fig. 8. While the shape of the convex hull is similar to that in the previous examples, the position of the center of gravity is different. By calculating $L^{(\mathrm{AB})}$, $L^{(\mathrm{BC})}$, and $L^{(\mathrm{CA})}$ in (15), we can see that $L^{(\mathrm{AB})} > 0$, $L^{(\mathrm{BC})} > 0$, and $L^{(\mathrm{CA})} > 0$ are satisfied. Therefore, even if the convex hull begins rotating about

an edge, the robot may not necessarily fall down. The region of GZMP is shown as a bold line in Fig. 8(c).

D. Continuous Motion

Let us consider the motion of a humanoid robot HRP-2, where its left hand handles an object placed on the table far from the robot. In such a case, a humanoid robot has to keep balance by using the interaction between the right hand and the table. The height and the weight of HRP-2 are 1.57 m and 57 kg, respectively. Let us consider the situation where both hands of a humanoid robot touch the table. When the left hand breaks contact with the table, the robot will fall down if the GZMP is not included in the region without considering the interaction between the left hand and the table.

The simulation results are shown in Figs. 9–11. As shown in Fig. 9(b) and (c), the body of HRP-2 moves to the right side before the left hand breaks contact with the table, and the robot always maintains its balance. Fig. 10 shows both the COP of the foot–ground contact and the GZMP trajectories. In Fig. 11, the position of the GZMP is calculated. When the left hand breaks contact ($t = 11.0$ s), the GZMP is included in the region without considering the interaction between the left hand and the table.

VI. Conclusion

In this paper, we studied the balance of a humanoid robot during manipulation tasks. We obtained the region of the GZMP for keeping balance of the robot by considering both the infinitesimal displacement and the moment about the edges of the 3-D convex hull of the supporting points. By using our proposed approach, we showed that the region of GZMP can be obtained for several cases of the manipulation tasks. We also showed the case where the convex polyhedron returns to the original configuration after it begins to rotate. The effectiveness of the proposed approach was confirmed by some simulation results.

In future work, we will consider constructing the motion generator of a humanoid robot, taking the GZMP into consideration. Also, we will construct another criterion for the robot to keep balance, taking the friction force into consideration.

Acknowledgment

The authors would like to express their sincere gratitude to Dr. K. Yokoi, Dr. F. Kanehiro, Mr. K. Fujiwara, and Dr. M. Morisawa, who are humanoid robotics researchers at AIST.

References

[1] M. Vukobratovic and J. Stepanenko, "On the stability of anthropomorphic systems," *Math. Biosci.*, vol. 15, pp. 1–37, 1972.

[2] A. Goswami, "Postural stability of biped robots and the foot rotation indicator (FRI) point," *Int. J. Robot. Res.*, vol. 19, no. 6, pp. 523–533, 1999.

[3] K. Yoneda and S. Hirose, "Tumble stability criterion of integrated locomotion and manipulation," in *Proc. IEEE/RSJ Int. Conf. Intell. Robots Syst.*, 1996, pp. 870–876.

[4] R. B. McGhee and A. A. Frank, "On the stability properties of quadruped creeping gaits," *Math. Biosci.*, vol. 3, pp. 331–351, 1968.

[5] E. G. Papadopoulos and D. A. Rey, "A new measure of tipover stability margin for mobile manipulators," in *Proc. IEEE Int. Conf. Robot. Autom.*, 1996, pp. 3111–3116.

[6] D. A. Messuri and C. A. Klein, "Automatic body regulation for maintaining stability of a legged vehicle during rough-terrian locomotion," *IEEE J. Robot. Autom.*, vol. RA-1, no. 3, pp. 132, 141, Jun. 1985.

[7] T. Kitagawa, K. Nagasaka, K. Nishiwaki, M. Inaba, and H. Inoue, "Generation of stand-up-motion with genetic algorithm for a humanoid," in *Proc. 17th Annu. Conf. RSJ*, 1999, pp. 1191–1192.

[8] T. Takenaka, "Walking Pattern Generation for a Legged Mobile Robot," Japanese Patent 3132156, May 27, 2001.

[9] ——, "Posture Control for a Legged Mobile Robot," Japanese Patent Appl. H10-230485, 1998.

[10] K. Hirai, M. Hirose, Y. Haikawa, and T. Takenaka, "The development of Honda humanoid robot," in *Proc. IEEE Int. Conf. Robot. Autom.*, 1998, pp. 1321–1326.

[11] S. Kagami, K. Nishiwaki, T. Sugihara, J. J. Kuffner, M. Inaba, and H. Inoue, "Design and implementation of software research platform for humanoid robotics: H6," in *Proc. IEEE/RSJ Int. Conf. Intell. Robots Syst.*, 2000, pp. 1559–1564.

[12] K. Kaneko, F. Kanehiro, S. Kajita, K. Yokoyama, K. Akachi, T. Kawasaki, S. Ota, and T. Isozumi, "Design of prototype humanoid robotics platform for HRP," in *Proc. IEEE/RSJ Int. Conf. Intell. Robots Syst.*, 2002, pp. 2431–2436.

[13] M. Fujita, Y. Kuroki, T. Ishida, and T. Doi, "Autonomous behavior control architecture of entertainment humanoid robot SDR-4X," in *Proc. IEEE/RSJ Int. Conf. Intell. Robots Syst.*, 2003, pp. 960–967.

[14] K. Inoue, H. Yoshida, T. Arai, and Y. Mae, "Mobile manipulation of humanoids—Real-time control based on manipulability and stability," in *Proc. IEEE Int. Conf. Robot. Autom.*, 2000, pp. 2217–2222.

[15] K. Harada, S. Kajita, K. Kaneko, and H. Hirukawa, "Pushing manipulation by humanoid considering two kinds of ZMPs," in *Proc. IEEE Int. Conf. Robot. Autom.*, 2003, pp. 1627–1632.

[16] K. Yokoyama, H. Handa, T. Isozumi, Y. Fukase, K. Kaneko, F. Kanehiro, Y. Kawai, F. Tomita, and H. Hirukawa, "Cooperative works by a human and a humanoid robot," in *Proc. IEEE Int. Conf. Robot. Autom.*, 2003, pp. 2985–2991.

[17] Y. Hwang, A. Konno, and M. Uchiyama, "Whole body cooperative tasks and static stability evaluations for a humanoid robot," in *Proc. IEEE/RSJ Int. Conf. Intell. Robots Syst.*, 2003, pp. 1901–1906.

[18] J. K. Salisbury and B. Roth, "Kinematics and force analysis of articulated hands," *ASME J. Mech. Transmissions, Autom., Des.*, vol. 105, pp. 33–41, 1982.

[19] V. Nguyen, "Constructing force closure grasps," *Int. J. Robot. Res.*, vol. 7, no. 3, pp. 3–16, 1988.

[20] K. Harada, M. Kaneko, and T. Tsuji, "Active force closure for multiple objects," *J. Robot. Syst.*, vol. 19, no. 3, pp. 133–141, 2002.

[21] K. M. Lynch, "The mechanics of fine manipulation by pushing," in *Proc. IEEE Int. Conf. Robot. Autom.*, 1992, pp. 2269–2276.

[22] K. Harada, H. Hirukawa, F. Kanehiro, K. Fujiwara, K. Kaneko, S. Kajita, and M. Nakamura, "Dynamical balance of a humanoid robot grasping an environment," in *Proc. IEEE/RSJ Int. Conf. Intell. Robots Syst.*, 2004, pp. 1167–1173.

[23] R. Mattikalli, D. Baraff, P. Khosla, and B. Repetto, "Gravitational stability of frictionless assemblies," *IEEE Trans. Robot. Autom.*, vol. 11, no. 3, pp. 374–388, Jun. 1995.

[24] T. Sugihara, Y. Nakamura, and H. Inoue, "Realtime humanoid motion generation through ZMP manipulation based on inverted pendulum control," in *Proc. IEEE Int. Conf. Robot. Autom.*, 2002, pp. 1404–1409.